Experimental Study of Ethanol and Helium Mixture Glow Discharge

S. Perusquía, P. G. Reyes, M. C. González, A. Gómez, H. Martínez, and J. Vergara

***Abstract*— This paper focuses on the study of a glow discharge generated from a mixture of ethanol (C_2H_6O) and helium (He). Plasma was generated at different concentrations of C_2H_6O and He gases maintained at a total pressure of 2 torr. We used optical emission spectroscopy (OES) to analyze the discharge mixture at different concentrations of He. The species identified by the OES technique correspond to O_2, CO^+, CO, H_β, H_α, and He. A single Langmuir probe was used to obtain the electron temperature (T_e) and electron density (n_e). T_e was found to be below 1.2 eV and n_e in the order of 10^{10} particles per cm^3.**

***Index Terms*— Ethanol, glow discharge, helium, optical emission spectroscopy (OES), single Langmuir probe.**

I. Introduction

AT THE present time, numerous contaminants are present in our environment; different forms of removing these compounds are one of the principal goals of research in several science areas. An example of those is ethanol (C_2H_6O) or ethyl alcohol (C_2H_5OH), which is a colorless and volatile chemical compound in the liquid state. It is obtained using ethylene via sulfuric acid hydrolysis. In its natural form, it is obtained by fermentation. In industry, C_2H_6O is used in antifreeze mixtures and in physiological and pathological specimens' preservation; it is used as a surgery antiseptic, a fuel, and a dissolvent for the synthesis of drugs, plastics, cosmetics, perfumes, and other products; furthermore, it is used to obtain acetaldehyde, vinegar, and butadiene [1]–[4]. It is a highly volatile compound and does not cause serious harm when inhaled in small amounts; however, inhalation of high concentration produces respiratory tract and eye irritation.

Another risk is that ethanol is flammable, causing explosive mixtures in closed areas. Therefore, C_2H_6O is classified as a volatile organic compound (VOC); VOCs are contaminants in the atmosphere and are interesting to study for their decomposition [5], [6]. Different methods can be employed for VOC decomposition such as bio-filtration, catalytic decomposition, thermic oxidation process, and plasma [7]–[9].

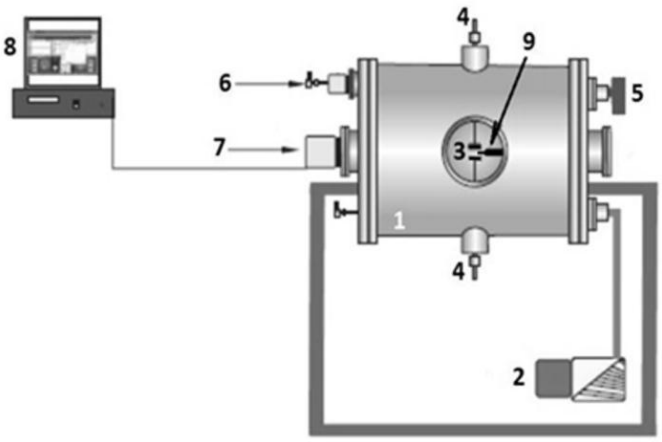

Fig. 1. Experimental setup.

Application of plasma technologies to study the decomposition of hydrocarbon has been gradually attracting attention. At low pressure, C_2H_6O has been studied by microwave (MW) plasma [10] and C_2H_6O–N_2 mixtures have been analyzed by dc plasma [11], whereas at atmospheric pressure plasma, C_2H_6O conversion has been studied by a dc atmospheric pressure discharge with a plasma cathode [12]. Hydrogen production from C_2H_6O in a nitrogen mixture has been investigated by MW plasma at atmospheric pressure [13].

In this paper, a C_2H_6O and helium (He) mixture plasma has been studied for film deposition via atmospheric pressure plasma deposition [14]. The results demonstrate that the treatment of different materials make possible a change in their hydrophilic properties.

The objective of this paper is to study the C_2H_6O–He mixture glow discharge produced at 2 torr by electrical characterization using a single Langmuir probe and by optical characterization using optical emission spectroscopy (OES).

II. Experimental Setup

The experimental device is the same from [15], as shown in Fig. 1, and it consists of the following.

1) Aluminum cylindrical vacuum chamber with a volume of 1.04×10^3 cm^3 (20 cm radius × 33 cm length).

Manuscript received October 3, 2016; revised July 19, 2018; accepted August 2, 2018. Date of publication August 20, 2018; date of current version January 8, 2019. This work was supported in part by the DGAPA under Project IN-102916 and in part by CONACyT under Project 225991 and Project 268644. The review of this paper was arranged by Senior Editor S. J. Gitomer. *(Corresponding author: H. Martínez.)*

S. Perusquía, P. G. Reyes, M. C. González, and A. Gómez are with the Facultad de Ciencias, Laboratorio de Física Avanzada, Instituto Literario 100, Universidad Autónoma del Estado de México, Toluca 50000, México (e-mail: perusquia@uaem.mx; grr.uaem@gmail.com; gonzalez@uamex.mx; agomez@uamex.com.mx).

H. Martínez is with the Laboratorio de Espectroscopia, Instituto de Ciencias Físicas, Universidad Nacional Autónoma de México, Cuernavaca 62210, México (e-mail: hm@fis.unam.mx).

J. Vergara is with the Laboratorio de Análisis y Sustentabilidad Ambiental, Instituto Profesional de la Región Oriente, Universidad Autónoma del Estado de Morelos, Xalostoc 62715, México (e-mail: vergara@uaem.mx).

Digital Object Identifier 10.1109/TPS.2018.2863716

2) Mechanical pump, which reach a base pressure of 1.0×10^{-3} torr.
3) Two movable copper electrodes with a diameter of 5 cm, positioned at the center of the vacuum chamber with 1 cm gap spacing.
4) Two electrical feedthroughs connected to the power supply (1 kW, Spellman SA4).
5) Pressure meter Pirani (MKS 103170027SH); the total pressure for the discharges in this paper was 2 torr.
6) Flowmeter (Matheson Tri. GasFM-1050); a continuous dynamic flow of C_2H_6O–He (ultrapure gas, PRAXAIR 99.99%) mixture was lit in the system though needle valves at desired pressures, while maintaining the total pressure of 2 torr; the concentration of the He gas in the mixture was done by changing the He partial pressure.
7) Optical emission system.
8) A computer with Ocean Optics software.
9) Single Langmuir probe.

To generate plasma, first, the vacuum chamber is evacuated with a mechanical pump; next, it is filled with the gases (C_2H_6O–He), and finally, the discharge is made between the electrodes at 420 V and 20 mA.

The OES consists of an optical fiber (solarization-resistant UV and fiber diameter size of 400 μm) that was connected to the entrance aperture of a high-resolution spectrometer (Ocean Optics, HR4000CG-UV-NIR). The inlet and outlet slits were 5 μm wide. The data were obtained in a single accumulation of 9-s integration time. The wavelength resolution was of 0.14 nm. The fiber optics assembly was positioned to collect the emission light appearing on the negative glow on the C_2H_6O–He mixture discharge.

The single Langmuir probe is an intrusive method to determine the plasma electron temperature and the electron density. It consists of a tungsten electrode with a diameter of 1 mm and length of 5.5 mm. This probe is connected to both a multimeter (Fluke 8846 A) and to a dc power supply (GW INSTEK GPR 30H100); the voltage range applied to the probe was between +300 V and −150 V.

III. Results

A. Electrical Characterization

I–V curve responses of the single Langmuir probe for different conditions, 100% He, 50% C_2H_6O + 50% He, and 100% C_2H_6O, at 2 torr are shown in Fig. 2. The electron temperature (T_e) and electron density (n_e) can be evaluated by the Druyvesteyn method [16]–[18]. The I–V trace is averaged over 20 sweeps. The ion current was subtracted from the total measurements current according to the method described by Gahan *et al.* [19]. The second derivate of the derivative of the probe current with respect to the probe voltage d^2I/dV^2 was obtained. The plasma potential φ_p was obtained from the zero-crossing point of d^2I/dV^2. The electron kinetic energy "ε" shown in (1) is simple equal to $\varphi_p - V_b$; V_b is the probe bias. Then, the electron energy distribution function (EEDF) f(ε) can be then calculated by the following expression:

$$f(E) = \frac{2\sqrt{2m_e}}{e^3 A}\frac{d^2 I_p}{dV^2} \tag{1}$$

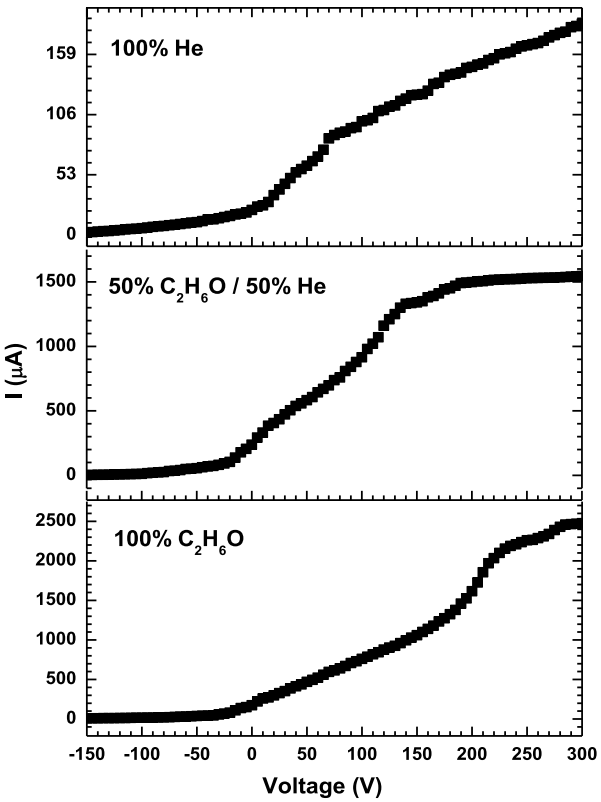

Fig. 2. Examples of I–V response of the single Langmuir probe for different mixture plasmas.

where e and m_e are the electron charge and electron mass, V and I_p are the applied voltage and current, and A is the probe area, respectively [20]. Then, the EEDF or F(E), n_e, and T_e are given as follows:

$$F(E) = \sqrt{E} f(E) \tag{2}$$

$$n_e = \int_0^\infty F(E)\, dE \tag{3}$$

$$T_e = \frac{2}{3n_e}\int_0^\infty E F(E)\, dE \tag{4}$$

where E is the electron energy.

In Fig. 3, the evolution of EEDF for different discharge conditions (100% He, 50% C_2H_6O + 50% He, and 100% C_2H_6O) versus the electron energy is plotted. The EEDF seems to be a Maxwellian distribution function for the 100% He, whereas at 50% C_2H_6O + 50% He and 100% C_2H_6O, the EEDF can be described as a two-temperature distribution of electrons with an excessive energy tail, which represents two groups of electrons with different energies. The first group, with low energy, affects the local electron densities and the local plasma conductance; the second group, with high energy, plays the main role in the local excitation and local ion production.

Furthermore, n_e, and T_e were evaluated using (3) and (4). The errors of these values are given by the standard deviation; in these cases, the results are 10% for both values. The electron density and electron temperature as a function of He % are plotted in Fig. 4. The values for T_e are in the range from 1.2 to 0.1 eV; this decrease as a function of the He % is attributed to a large amount of active species that it can be produced from the reaction of electron and molecules,

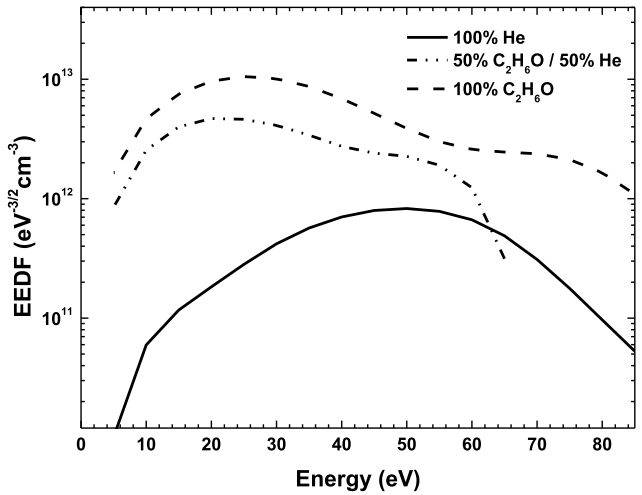

Fig. 3. EEDF for the 100% He, 50% C_2H_6O + 50% He, and 100% C_2H_6O discharges.

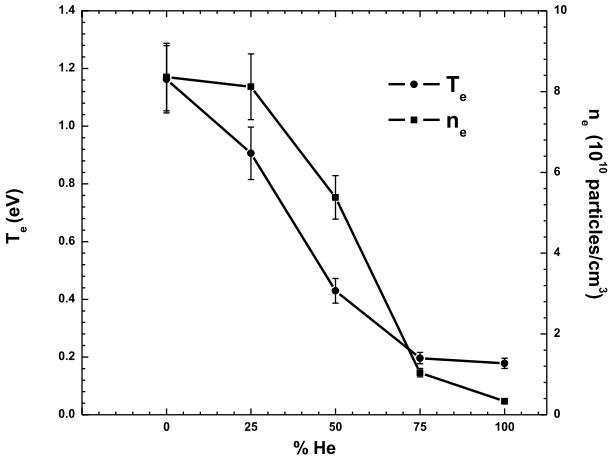

Fig. 4. T_e and n_e as a function of He %.

resulting in the decomposition of C_2H_6O. Among them, the fast reactions

$$C_2H_6O + O \rightarrow C_2H_5O + OH \quad (5)$$

$$C_2H_6O + OH \rightarrow C_2H_5O + H_2O. \quad (6)$$

Other reactions occurring between C_2H_6O molecules and electrons directly mainly include

$$C_2H_6O + e \rightarrow CH_3 + CH_2OH + e \quad (7)$$

$$C_2H_6O + e \rightarrow C_2H_5 + OH + e \quad (8)$$

$$C_2H_6O + e \rightarrow C_2H_5OH^+ + 2e. \quad (9)$$

The reduction of He influences the dissociation of C_2H_6O production, producing a reduction in the mean free path (λ) and an increase in the frequency of collision (υ), and generating a reduction of the electron temperature (T_e).

On the other hand, the values for n_e are between 8.3 × 10^{10} and 3.3 × 10^{10} particles per cm^3. The decrease of n_e as a function of He % (see Fig. 4) is due to the decrease of C_2H_6O content in the mixture; the electron impact dissociation of ground state C_2H_6O molecules increases the number of free electrons; then the C_2H_6O discharge has more electron density than the mixture discharges.

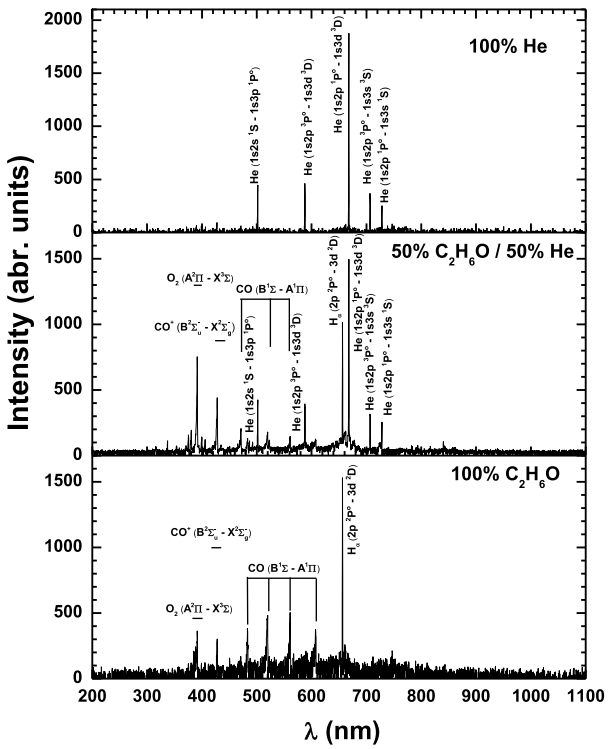

Fig. 5. OES of ethanol and He mixture glow discharge.

The measurements of the electron temperature T_e in the range of 0.18–1.16 eV and an ion density of n_i between (0.33–8.36) × 10^{16} m^{-3} imply that the Debye length λ_D for these plasmas is between 0.021 and 0.054 mm, which is small compared to the probe radius of 0.5 mm, a condition that is called the transition sheath region [21], so for probe operation the present plasma is collisionless.

B. OES Measurements

Fig. 5 shows the optical emission spectra of all the glow discharges studied in this paper. The species observed and identified [22] were at 391.4 nm for O_2 ($A^2\Pi - X^2\Sigma$) Comet–Tail system; at 427.73 nm for CO^+ ($B^3\Sigma_u^- - X^3\Sigma_g^-$) Schumann–Runge system; at 483.53, 518.85, 561.02, and 606.99 nm for CO ($B^1\Sigma - A^1\Pi$) Angstrom system; at 486.13 nm for H_β; at 656.27 nm for H_α; and at 501.56, 587.59, 667.96, 706.57, and 728.13 nm for He.

A well-known method for electron temperature estimation consists in using the spectroscopy diagnostic method, which is based on determining the relative intensities of the two spectral lines of the same atom. This method assumes that the velocity distributions of the electrons are Maxwellian, and the population of the emitting levels follows the Boltzmann distribution. Explicitly, the formula is

$$T_e = \frac{E_2 - E_1}{k} \left(\ln \left[\frac{I_1 \lambda_1 g_2 A_2}{I_2 \lambda_2 g_1 A_1} \right] \right)^{-1}. \quad (10)$$

The index "1" refers to the first spectral line, "2" to the second spectral line, k is the Boltzmann's constant, I_i the intensity of the lines measure by OES, λ_i is the wavelength of the emitted line, E_i the energy of the excited state, g_i its statistical weight, and A_i is the Einstein transition probability

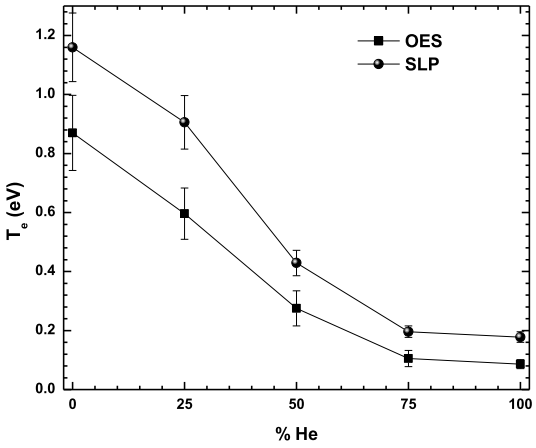

Fig. 6. T_e as a function of He %.

for spontaneous emission. In these cases, the values for the energy, the degeneracy, and the values for the Einstein transition probability are taken of the NIST Atomic Spectra Database Lines Form [23]. The lines used to evaluate the electron temperature were He 667.96 and He 706.57 nm in the C_2H_6O–He mixture discharges; and, H_α 656.27 and H_β 486.13 nm for 100% C_2H_6O discharge. The errors for this calculate are obtained from the standard deviation (10%). Fig. 6 shows the variation of the T_e as a function of %He at 2 torr pressure and compared with the values obtained by single Langmuir probe. The graph shows that T_e in both methods decreases with the increase in %He in the mixture. It is worth noting that T_e measured by the single Langmuir probe is greater than the T_e measured by OES, but both have similar trends. This fact may be explained in terms of contamination of the probe [24] and bi-Maxwellian nature of the plasma; under such conditions, the Langmuir probe and OES results do not match [25]. Moreover, the difference between the two temperatures may be explained because the probe measurements are localized, whereas OES yields average results.

The electron density was estimated using the Stark broadened spectral line profile, since it depends on the local charge density. The Balmer-alpha line H_α has been measured in the present experiment. The H_α line profiles have been fit by a Voigt profile. A deconvolution procedure has been used to determine the full width at half-maximum of the Gaussian ($\Delta\lambda_G$) and Lorentzian ($\Delta\lambda_L$) components. Stark and van der Waals effects contribute to the Lorentzian broadening under the present conditions. To estimate the van der Waals broadening, we adopted the expression presented in [26], along with the measured gas temperature Tg. The calculated van der Waals broadening values (0.11–0.13 Å) have been deconvoluted from the Lorentzian full width at half-maximum to obtain the Stark broadening. n_e has been evaluated, making a fit of the widths provided by Gigosos *et al.* [27] for a reduced mass of 0.8, which corresponds to the pair emitter-perturbed condition, i.e., the pair H–He.

Fig. 7 displays n_e as a function of %He and compares it with the values obtained by a single Langmuir probe. It can be observed that n_e in both methods decreases with the increase in %He in the mixture. n_e measured by the single Langmuir

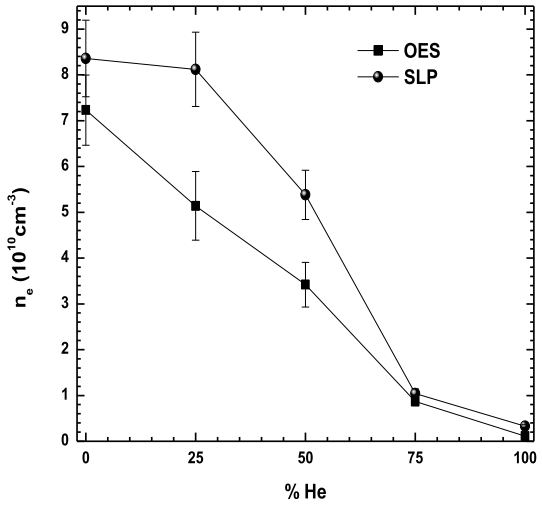

Fig. 7. n_e as a function of He %.

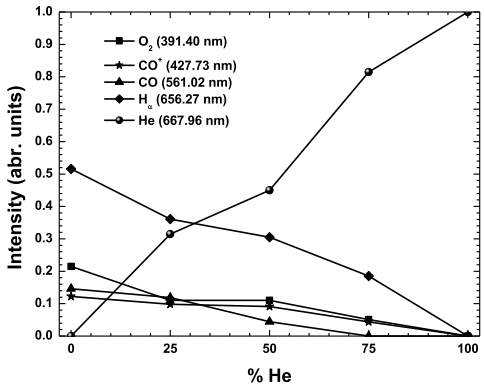

Fig. 8. Intensity of the most intense lines and bands observed in the mixture glow discharge as a function of He %.

probe is greater than the n_e measured by OES, but both have similar trends. This fact may be explained in the same form given before by the T_e.

Furthermore, the changes of the intensity of the most intense peaks as a function of He % are plotted in Fig. 8. The introduction of C_2H_6O vapor (even a small amount) into the He plasma significantly changes the character of the emission spectrum of the generated plasma. It can be noted that hydrogen is the main product obtained from C_2H_6O decomposition. The hydrogen production is almost 50% of the fragment products. The bands of O_2 (391.4 nm), CO^+ (427.73 nm), and CO (561.02 nm), and the line H_α (656.27 nm) decrease with increasing He content, whereas the He lines (667.96 nm) increase. The difference in population of this species may be due to their different excitations and ionization energies and the increase of He metastable states He I (501.56, 587.59, 667.96, 706.57, and 728.13 nm) in the discharge.

Fig. 3 shows the calculated EEDFs for C_2H_6O, He, and He–C_2H_6O mixture. It is shown that the EEDF (5–30 eV) is defined by excitation and ionization of He atoms, and the excitation, ionization, and dissociation of C_2H_6O molecules by electron collision, generating the following atomic and molecular reactions in the C_2H_6O–He mixture:

$$e^- + He \rightarrow He^* + e \quad (11)$$

$$e^- + He \rightarrow He^+ + 2e \quad (12)$$

$$e^- + C_2H_5OH \rightarrow C_2H_6 + O + e \quad (13)$$

$$e^- + C_2H_5OH \rightarrow C_2H_4 + H_2O + e \quad (14)$$

$$e^- + C_2H_5OH \rightarrow C_2H_5 + OH + e \quad (15)$$

$$e^- + OH \rightarrow O + H + e \quad (16)$$

$$e^- + C_2H_5OH \rightarrow CH_3 + CH_2 + OH + e \quad (17)$$

$$e^- + CH_2 \rightarrow C + H_2 + e. \quad (18)$$

Equation (11) corresponds to He excitation, (12) corresponds to He ionization, and (13)–(18) correspond to the several dissociation processes. These reactions produced the species observed by OES (Fig. 5). Also, the EEDF calculated involved electron energies to produce higher He metastable states, as can be seen from OES measurements, which contributes to the decomposition of the C_2H_6O by the inelastic collisions of Helium metastable atoms through penning reactions by [28], [29]

$$C_2H_6O + He^* \rightarrow C_2H_5O + H + He \quad (19)$$

$$C_2H_6O + He^* \rightarrow C_2H_5 + OH + He \quad (20)$$

which produces the products H and OH observed by OES measurements.

The changes of the intensity of the most intense peaks as a function of %He (Fig. 8) can be explained by the behavior observed in the EEDF calculation. The processes involving He atoms most strongly affect the EEDF, as can be seen in Fig. 3. The presence of He in the mixture EEDF describes two temperature distributions of electrons with an excessive energy tail.

IV. Conclusion

Decomposition of the C_2H_6O molecule was achieved and the lines and bands observed by OES were O_2 ($A^2\Pi - X^2\Sigma$), CO^+ ($B^3\Sigma_u^- - X^3\Sigma_g^-$), CO ($B^1\Sigma - A^1\Pi$), H_β, H_α, and He. The formation of the hydrogen atoms H_α and CO^+ and CO molecules can be attributed to the electron impact dissociation of C_2H_6O.

The electron density and the electron temperature were evaluated using a single Langmuir probe datum. T_e was found in the range of 1.2–0.1 eV and in the order of 10^{10} particles per cm^3. To dissociate different gases, including the VOC, the glow discharge is an efficient method because the plasma generated has a higher chemical reactivity.

Acknowledgment

The authors would like to thank N. Rodriguez from the Facultad de Ciencias de la Universidad Autónoma del Estado de México, Toluca, Mexico, and H. H. Hinojosa, F. Castillo, and O. Flores from the Instituto de Ciencias Físicas, Universidad Nacional Autónoma de México, Mexico City, Mexico, for their technical assistance.

References

[1] D. S. Levko, A. N. Tsymbalyuk, and A. I. Shchedrin, "Plasma kinetics of ethanol conversion in a glow discharge," *Plasma Phys. Rep.*, vol. 38, no. 11, pp. 913–921, 2012.

[2] F. Chen, X. Huang, D. Cheng, and X. Zhan, "Hydrogen production from alcohols and ethers via cold plasma: A review," *Int. J. Hydrogen Energy*, vol. 39, no. 17, pp. 9036–9046, 2014.

[3] X. Zhu, T. Hoang, L. L. Lobban, and R. G. Mallinson, "Partial oxidation of ethanol using a non-equilibrium plasma," *Int. J. Hydrogen Energy*, vol. 39, no. 17, pp. 9047–9056, 2014.

[4] J. Brust, "Ethanol and cognition: Indirect effects, neurotoxicity and neuroprotection: A review," *Int. J. Environ. Res. Public Health*, vol. 7, pp. 1540–1557, Apr. 2010.

[5] A. Daneshkhah, S. Shrestha, M. Agarwal, and K. Varahramyan, "Poly (vinylidene fluoride-hexafluoropropylene) composite sensors for volatile organic compounds detection in breath," *Sens. Actuators B, Chem.*, vol. 221, pp. 635–643, Dec. 2015.

[6] S. Öztürk, A. Kösemen, Z. A. Kösemen, N. Kilinç, Z. Z. Öztürk, and M. Penza, "Electrochemically growth of Pd doped ZnO nanorods on QCM for room temperature VOC sensors," *Sens. Actuators B, Chem.*, vol. 222, pp. 280–289, Jan. 2016.

[7] J. S. Chang, "Recent development of plasma pollution control technology: A critical review," *Sci. Technol. Adv. Mater.*, vol. 2, pp. 571–576, Jan. 2001.

[8] M. Hrabovsky *et al.*, "Gasification of biomass in water/gas-stabilized plasma for syngas production," *Czechoslovak J. Phys.*, vol. 56, pp. B1199–B1206, Oct. 2006.

[9] S. Fukahori, I. Yumi, H. Ichiura, T. Kitaoka, T. Tanaka, and H. Wariishi, "Effect of void structure of photocatalyst paper on VOC decomposition," *Chemosphere*, vol. 66, no. 11, pp. 2136–2141, 2007.

[10] S. Bing, B. Wang, X. M. Zhu, Z. Y. Yan, Y. J. Liu, and H. Liu, "Study on the emission spectrum of hydrogen production with microwave discharge plasma in ethanol solution," *Spectrosc. Spectral Anal.*, vol. 36, no. 3, pp. 823–826, 2016.

[11] D. T. Usmanov, L. C. Chen, K. Hiraoka, H. Wada, H. Nonamie, and S. Yamabef, "Nitrogen incorporation in saturated aliphatic C6–C8 hydrocarbons and ethanol in low-pressure nitrogen plasma generated by a hollow cathode discharge ion source," *J. Mass Spectrometry*, vol. 51, pp. 446–452, Jun. 2016.

[12] V. I. Arkhipenko, A. A. Kirillov, L. V. Simonchik, Y. A. Safronau, A. P. Chernukho, and A. N. Migoun, "Atmospheric pressure glow discharge in air used for ethanol conversion: Experiment and modelling," *Open Chem.*, vol. 13, no. 1, pp. 292–296, 2016.

[13] B. Hrycak, D. Czylkowski, R. Miotk, M. Dors, M. Jasinski, and J. Mizeraczyk, "Hydrogen production from ethanol in nitrogen microwave plasma at atmospheric pressure," *Open Chem.*, vol. 13, pp. 317–324, Jan. 2015.

[14] K.-S. Chen *et al.*, "The film deposition via atmospheric pressure plasma from ethanol and He mixing gases," *Surf. Coat. Technol.*, vol. 231, pp. 408–411, Sep. 2013.

[15] J. Torres, P. G. Reyes, C. Torres, H. Martínez, and J. Vergara, "Optical emission spectroscopy of H_γ, H_α, and H_β in a glow discharge mixture of Ar/H_2," *IEEE Trans. Plasma Sci.*, vol. 43, no. 3, pp. 846–850, Mar. 2015.

[16] N. Kang, S.-G. Oh, and A. Ricard, "Determination of the electron temperature in a planar inductive argon plasma with emission spectroscopy and electrostatic probe," *J. Phys. D: Appl. Phys.*, vol. 41, no. 15, p. 155203, 2008.

[17] V. A. Godyak, R. B. Piejak, and B. M. Alexandrovich, "Probe diagnostics of non-Maxwellian plasmas," *J. Appl. Phys.*, vol. 73, no. 8, pp. 3657–3663, 1993.

[18] T. H. Chung, H. R. Kang, and M. K. Bae, "Optical emission diagnostics with electric probe measurements of inductively coupled Ar/O_2/Ar-O_2 plasmas," *Phys. Plasmas*, vol. 19, no. 11, p. 113502, 2012.

[19] D. Gahan, B. Dolinaj, and M. B. Hopkins, "Comparison of plasma parameters determined with a Langmuir probe and with a retarding field energy analyzer," *Plasma Sources Sci. Technol.*, vol. 17, no. 3, p. 035026, 2008.

[20] H. J. Roh *et al.*, "Determination of electron energy probability function in low-temperature plasmas from current—Voltage characteristics of two Langmuir probes filtered by Savitzky–Golay and Blackman window methods," *Current Appl. Phys.*, vol. 15, no. 10, pp. 1173–1183, 2015.

[21] K. U. Riemann, "The influence of collisions on the plasma sheath transition," *Phys. Plasmas*, vol. 4, no. 11, pp. 4158–4166, 1997.

[22] (2016). *NIST: Atomic Spectra Database Lines Form*. National Institute of Standards and Technology. Accessed: Mar. 15, 2016. [Online]. Available: http://physics.nist.gov/PhysRefData/Handbook/Tables/heliumtable1.htm

[23] *NIST: Atomic Spectra Database Lines Form*. National Institute of Standards and Technology. Accessed: Jul. 30, 2018. [Online]. Available: http://physics.nist.gov/PhysRefData/ASD/lines_form.html

[24] E. Stamate and K. Ohe, "Influence of surface condition in Langmuir probe measurements," *J. Vac. Sci. Technol. A, Vac., Surf., Films*, vol. 20, no. 3, pp. 661–666, 2002.
[25] N. C. M. Fuller, M. V. Malyshev, V. M. Donnelly, and I. P. Herman, "Characterization of transformer coupled oxygen plasmas by trace rare gases-optical emission spectroscopy and Langmuir probe analysis," *Plasma Sources Sci. Technol.*, vol. 9, no. 2, p. 116, 2000.
[26] C. Oliveira, J. A. Souza, M. P. Gomes, B. N. Sismanoglu, and J. Amorim, "Hyperthermal hydrogen atoms in argon-hydrogen atmospheric pressure microplasma jet," *Appl. Phys. Lett.*, vol. 93, no. 4, p. 041503, 2008.
[27] M. A. Gigosos, M. Á. González, and V. Cardeñoso, "Computer simulated Balmer-alpha, -beta and -gamma Stark line profiles for non-equilibrium plasmas diagnostics," *Spectrochim. Acta B, At. Spectrosc.*, vol. 58, no. 8, pp. 1489–1504, 2003.
[28] D. Levko, A. Shchedrin, V. Chernyak, S. Olszewski, and O. Nedybaliuk, "Plasma kinetics in ethanol/water/air mixture in a 'tornado'-type electrical discharge," *J. Phys. D: Appl. Phys.*, vol. 44, no. 14, p. 145206, 2011.
[29] D. Levko, A. Sharma, and L. L. Raja, "Non-thermal plasma ethanol reforming in bubbles immersed in liquids," *J. Phys. D: Appl. Phys.*, vol. 50, no. 8, p. 085202, 2017.

Authors' photographs and biographies not available at the time of publication.